

Constraints on axion-nucleon coupling constants from measuring the Casimir force between corrugated surfaces

V. B. Bezerra,¹ G. L. Klimchitskaya,^{2,3,1} V. M. Mostepanenko,^{2,3,1} and C. Romero¹

¹*Department of Physics, Federal University of Paraíba,
C.P.5008, CEP 58059-970, João Pessoa, Pb-Brazil*

²*Central Astronomical Observatory at Pulkovo of the
Russian Academy of Sciences, St.Petersburg, 196140, Russia*

³*Institute of Physics, Nanotechnology and Telecommunications,
St.Petersburg State Polytechnical University, St.Petersburg, 195251, Russia*

Abstract

We obtain stronger laboratory constraints on the coupling constants of axion-like particles to nucleons from measurements of the normal and lateral Casimir forces between sinusoidally corrugated surfaces of a sphere and a plate. For this purpose, the normal and lateral additional force arising in the experimental configurations due to two-axion exchange between protons and neutrons are calculated. Our constraints following from measurements of the normal and lateral Casimir forces are stronger than the laboratory constraints reported so far for masses of axion-like particles larger than 11 eV and 8 eV, respectively. A comparison between various laboratory constraints on the coupling constants of axion-like particles to nucleons obtained from the magnetometer measurements, Eötvös- and Cavendish-type experiments, and from the Casimir effect is performed over the wide range of masses of axion-like particles from 10^{-10} eV to 20 eV.

PACS numbers: 14.80.Va, 12.20.Fv, 14.80.-j

I. INTRODUCTION

After the publication of the papers by Peccei and Quinn [1], Weinberg [2] and Wilczek [3], light pseudoscalar particles named axions have become the subject of active theoretical and experimental investigations. This is because there is no other natural explanation for the absence of large CP violation and respective electric dipole moment of the neutron in strong interactions predicted by quantum chromodynamics (QCD). In addition, axions reasonably explain the nature of dark matter in astrophysics [4, 5] which makes them of prime importance for our general physical concepts.

A lot of experiments on searching axions have been performed (see Refs. [6–10] for a review), but the detection was not succeeded yet. After the originally introduced QCD axions were constrained to a very narrow band of parameter space, many kinds of axion-like particles have been discussed in the framework of Grand Unified Theory (GUT) and string theory [10]. Specifically, much attention has been given to the models of GUT (DFSZ) axions [11, 12] and the so-called *hadronic* (KSVZ) axions [13, 14]. The latter model involves a relationship between the axion-nucleon coupling constant and the breaking scale of the Peccei-Quinn symmetry and, in its turn, falls into several groups of models (see, e.g., Refs. [15, 16]).

Axion-like particles can interact with photons, electrons and nucleons. These interactions are used for experimental searches of axion-like particles in both the laboratory experiments (see below) and in astrophysics (see, for instance, constraints on the axion-photon and axion-electron coupling constants obtained by means of axion solar telescope [17] and from the Compton process and electron-positron annihilation with an axion emission in stellar plasmas [18, 19], respectively). Both the laboratory and astrophysical constraints may depend on the model of axions used containing different relations between couplings to different particles (for instance, the constraints from the solar axion data [20, 21] and from the neutrino data of supernova SN 1987A [22] are found using the model of hadronic axions, where the coupling constant is a function of the axion mass). The astrophysical constraints may also depend on complicated behavior of matter in stars. For example, the coupling constants of hadronic axions to nucleons, obtained [23, 24] from an axion emission rate during stellar cooling, depend [24] on significant uncertainties in the dense nuclear matter effects. Furthermore, the astrophysical constraints could depend on the environment [25–27]. This is the reason why the constraints following from the table-top laboratory experiments, which avoid

such kind uncertainties and applicable to a wide range of axion-like particles, are of much interest for axion physics. At the same time it is necessary to stress that the astrophysical constraints are often much stronger than the laboratory limits. Thus, from the solar axion data the upper limits for axion mass $m_a \leq 159$ eV [20] and $m_a \leq 145$ eV [21] were obtained. From the neutrino data of supernova SN 1987A and from stellar cooling by the emission of hadronic axions the coupling constant of axions to nucleons was found to be less or of order 10^{-10} [22–24].

In Ref. [28] the model-independent constraints on an axion-neutron coupling constants were found with the help of a magnetometer using spin-polarized atoms. These constraints are the strongest for m_a from 10^{-10} to 6×10^{-6} eV. In Ref. [29] the constraints on an axion-nucleon coupling constants were obtained from the laboratory experiments of Eötvös [30, 31] and Cavendish [32, 33] type for m_a from 10^{-9} to 10^{-5} eV. Keeping in mind that the test bodies in these experiments were unpolarized, any additional force could come from the two-axion exchange between nucleons belonging to different test bodies. Using the same approach, stronger constraints on the axion-nucleon coupling constants were obtained in Ref. [34] from the results of more modern Cavendish-type experiment [35] in the region of axion masses from 10^{-6} to 10^{-2} eV. The additional force arising due to two-axion exchange between nucleons was then used [36–38] to constrain the axion-nucleon coupling constants from experiments on measuring the Casimir-Polder [39] and Casimir [40–46] interactions. This allowed to strengthen the laboratory constraints on the coupling constants of axion-like particles to nucleons in the wide range of their masses from 10^{-3} eV to 15 eV.

The previously obtained constraints on axion-like particles from the Casimir effect [36–38] used experiments with either plane or spherical boundary surfaces. There is, however, another class of experiments on measuring the Casimir force exploiting test bodies with corrugated surfaces. The normal Casimir force between a smooth Au-coated sphere and a rectangular corrugated Si plate was measured and found in agreement with the scattering theory in Refs. [47–49]. The use of Si, whose density is smaller than of Au, does not allow to get strongest constraints on axions using the data of these experiments. The normal Casimir force between sinusoidally corrugated Au-coated surfaces of a sphere and a plate was measured in Ref. [50] and also found in agreement with computations using the scattering theory. This experiment is rather promising for constraining the coupling constants of axion-like particles to nucleons. In the experiments of Refs. [51, 52] the lateral Casimir force acting

in tangential direction to the sinusoidally corrugated Au-coated surfaces of a sphere and a plate has been measured. The comparison with computational results using the scattering theory demonstrated a very good agreement with the measurement data [51, 52]. Thus, these experiments are also of high promise for obtaining new constraints on the interaction of axion-like particles with nucleons.

In this paper, we obtain the constraints on the coupling constants of axion-like particles to nucleons using the measure of agreement with theory of the experimental data of Refs. [50–52] exploiting the corrugated Au-coated surfaces of a sphere and a plate. For this purpose, we calculate the additional normal and lateral forces arising between the sinusoidally corrugated surfaces of a sphere and a plate due to two-axion exchange. The constraints are found from the fact that these forces were not observed in the limits of experimental error. They are shown to be the strongest laboratory constraints in the region of masses of axion-like particles from 8 to 20 eV. This conclusion is obtained from the comparison with other laboratory constraints on the coupling constants of axion-like particles to nucleons obtained in the literature for m_a larger than 10^{-10} eV.

The paper is organized as follows. In Sec. II we calculate the additional normal force due to two-axion exchange between the sinusoidally corrugated bodies and derive the constraints on the coupling constants of axion-like particles to nucleons from the experimental data of Ref. [50]. Section III contains the derivation of the additional lateral force due to exchange of two axion-like particles. The respective constraints are found from the measurement data of Refs. [51, 52]. In Sec. IV we present the comparison of our results with other laboratory constraints obtained in the literature. Section V contains our conclusions and discussion.

Throughout the paper we use units in which $\hbar = c = 1$.

II. CONSTRAINTS FROM MEASURING THE NORMAL CASIMIR FORCE BETWEEN SINUSOIDALLY CORRUGATED SURFACES

In Ref. [50] the normal Casimir force was measured between a sinusoidally corrugated Au-coated plate and a sinusoidally corrugated Au-coated sphere at various angles between the uniaxial corrugations from 0° to 2.4° using an atomic force microscope (AFM). In what follows, we use the measurement data for parallel corrugation axes. The plate was the diffraction grating with uniaxial sinusoidal corrugations of period $\Lambda = 570.5$ nm and ampli-

tude $A_1 = 40.2$ nm. The side of the plate was equal to 1 cm allowing to consider it infinitely large. The grating was made of a hard epoxy with density $\rho_e = 1.08$ g/cm³ and coated with an Au layer of thickness $\Delta_{\text{Au}}^{(1)} = 300$ nm. The corrugations on the bottom surface of a polystyrene sphere of density $\rho_p = 1.06$ g/cm³ were imprinted under pressure from the plate. For technological purposes the sphere was coated with a layer of Cr of thickness $\Delta_{\text{Cr}}^{(2)} = 10$ nm, then with a layer of Al of thickness $\Delta_{\text{Al}}^{(2)} = 20$ nm, and finally with a layer of Au of thickness $\Delta_{\text{Au}}^{(2)} = 110$ nm. The outer radius of the coated sphere was measured to be $R = 99.6$ μ m. The imprinted corrugations on the sphere have had the same period as on the plate and the amplitude $A_2 = 14.6$ nm. The size of the imprint area was $L_x \approx L_y \approx 14$ μ m, i.e., much larger than the corrugation period Λ .

A. Calculation of the normal force due to exchange of two axion-like particles

Now, let us calculate the normal (i.e., perpendicular to the mean levels of boundary surfaces) force acting between a sinusoidally corrugated spherical envelope of thickness d_2 and a sinusoidally corrugated plate of thickness d_1 due to exchange of two axion-like particles between protons and neutrons belonging to them. We assume the pseudoscalar character of an axion-fermion coupling and neglect the axion-electron interaction [29]. The account of the latter and possible scalar axion-fermion coupling [53] could lead to only a minor strengthening of the obtained constraints.

The pseudoscalar interaction of axions a with fermions ψ is described by the Lagrangian

$$\mathcal{L}_{\text{ps}} = -ig_{ak}\bar{\psi}\gamma_5\psi a, \quad (1)$$

where g_{ak} is the coupling constant for an axion to a proton ($k = p$) or to a neutron ($k = n$). Note that the originally introduced QCD axions are pseudo Nambu-Goldstone bosons and their interaction with fermions is described by the pseudovector interaction Lagrangian

$$\mathcal{L}_{\text{pv}} = \frac{g_{ak}}{2m_a}\bar{\psi}\gamma_5\gamma_\mu\psi\partial^\mu a. \quad (2)$$

Both the pseudoscalar and pseudovector Lagrangians (1) and (2) result in one and the same action after the integration by parts is performed. However, the quantum field theory with the pseudoscalar Lagrangian (1) is renormalizable, whereas it is nonrenormalizable with the pseudovector Lagrangian (2). This may result in some nonequivalence [7, 9]. Below we

assume the pseudoscalar interaction (1) which is applicable to a wide class of axion models, specifically, to all GUT axion-like particles [53].

First, we consider two plane parallel plates of infinitely large area with thicknesses d_1 and d_2 . Let the coordinate plane x, y coincide with an upper surface of the lower plate, and the z axis be perpendicular to it. Let z be the varying separation distance between the plates. Using the pseudoscalar Lagrangian (1), the effective interaction potential due to exchange of two axion-like particles between two nucleons situated at the points \mathbf{r}_1 of the lower plate and \mathbf{r}_2 of the upper plate has the form [29, 54, 55]

$$V_{kl}(|\mathbf{r}_1 - \mathbf{r}_2|) = -\frac{g_{ak}^2 g_{al}^2}{32\pi^3 m^2} \frac{m_a}{(\mathbf{r}_1 - \mathbf{r}_2)^2} K_1(2m_a |\mathbf{r}_1 - \mathbf{r}_2|). \quad (3)$$

Here, $k, l = p$ for protons and $k, l = n$ for neutrons, $m = (m_p + m_n)/2$ is the mean nucleon mass, and $K_1(z)$ is the modified Bessel function of the second kind. Equation (3) is valid under the assumption $|\mathbf{r}_1 - \mathbf{r}_2| \gg 1/m$ which is fulfilled with a large safety margin due to the fact that in measurements of Ref. [50] the interacting bodies are separated by more than 127 nm.

The interaction energy per unit area of two plane parallel plates due to two-axion exchange is given by

$$E(z) = 2\pi \sum_{k,l} n_{k,1} n_{l,2} \int_z^{z+d_1} dz_1 \int_{-d_2}^0 dz_2 \int_0^\infty \rho d\rho \times V_{kl}(\sqrt{\rho^2 + (z_1 - z_2)^2}), \quad (4)$$

where V_{kl} is defined in Eq. (3) and

$$n_{p,i} = \frac{\rho_i}{m_H} \frac{Z_i}{\mu_i}, \quad n_{n,i} = \frac{\rho_i}{m_H} \frac{N_i}{\mu_i}. \quad (5)$$

The index $i = 1, 2$ here numerates the lower and upper plates, respectively, $\rho_{1,2}$ are the densities of plate materials, $Z_{1,2}$ and $N_{1,2}$ are the numbers of protons and the mean numbers of neutrons in the atoms (molecules) of the plates. The quantities $\mu_{1,2}$ are defined as $\mu_{1,2} = m_{1,2}/m_H$, where $M_{1,2}$ and m_H are the mean masses of the atoms (molecules) of the plate materials and the mass of the atomic hydrogen, respectively. In Ref. [56] one can find the tabulated values of Z/μ and N/μ for the first 92 elements of the Periodic Table taking into account their isotopic composition.

Substituting Eqs. (3) and (5) into Eq. (4), one obtains

$$E(z) = -\frac{m_a}{m^2 m_H^2} C_1 C_2 \int_z^{z+d_1} dz_1 \int_{-d_2}^0 dz_2 \int_0^\infty \rho d\rho \times \frac{K_1(2m_a \sqrt{\rho^2 + (z_1 - z_2)^2})}{\rho^2 + (z_1 - z_2)^2}, \quad (6)$$

where

$$C_i = \rho_i \left(\frac{g_{ap}^2}{4\pi} \frac{Z_i}{\mu_i} + \frac{g_{an}^2}{4\pi} \frac{N_i}{\mu_i} \right). \quad (7)$$

It is convenient to use the integral representation [57]

$$\frac{K_1(t)}{t} = \int_1^\infty du \sqrt{u^2 - 1} e^{-tu} \quad (8)$$

and the new variable $v = \sqrt{\rho^2 + (z_1 - z_2)^2}$. Then Eq. (6) can be rearranged to

$$E(z) = -\frac{C_1 C_2}{4m_a m^2 m_H^2} \int_1^\infty du \frac{\sqrt{u^2 - 1}}{u^3} e^{-2m_a u z} \times (1 - e^{-2m_a u d_1})(1 - e^{-2m_a u d_2}). \quad (9)$$

Now we assume that the opposite sides of the plates under consideration are covered with uniaxial sinusoidal corrugations of equal period Λ . There was no phase shift between corrugations on both bodies in the experiment of Ref. [50]. The corrugation axes are directed along the axis y . Then, the separation distance between the surfaces of the plates is given by

$$z \equiv z(x) = a + (A_1 - A_2) \cos \frac{2\pi x}{\Lambda}, \quad (10)$$

where a is the separation distance between the mean levels of corrugations on both plates. The interaction energy due to two-axion exchange per unit area of corrugated plates can be obtained by the method of geometrical averaging [58, 59]

$$E_{\text{corr}}(a) = \frac{1}{\Lambda} \int_0^\Lambda dx E(z(x)), \quad (11)$$

where $E(z)$ and $z(x)$ are defined in Eqs. (9) and (10), respectively. For the Casimir forces, Eq. (11) is an approximate one and works good under the condition $\Lambda \gg a$ [51, 52]. However, for the Yukawa-type forces and forces due to two-axion exchange it is, in fact, exact. Substituting Eqs. (9) and (10) in Eq. (11), one arrives at

$$E_{\text{corr}}(a) = -\frac{C_1 C_2}{4m_a m^2 m_H^2 \Lambda} \int_0^\Lambda dx \int_1^\infty du \frac{\sqrt{u^2 - 1}}{u^3} \times e^{-2m_a u a} e^{-2m_a u (A_1 - A_2) \cos(2\pi x / \Lambda)} \times (1 - e^{-2m_a u d_1})(1 - e^{-2m_a u d_2}). \quad (12)$$

The integration with respect to x results in

$$\begin{aligned}
E_{\text{corr}}(a) = & -\frac{C_1 C_2}{4m_a m^2 m_H^2} \int_1^\infty du \frac{\sqrt{u^2 - 1}}{u^3} \\
& \times e^{-2m_a u a} I_0(2m_a u (A_1 - A_2)) \\
& \times (1 - e^{-2m_a u d_1})(1 - e^{-2m_a u d_2}),
\end{aligned} \tag{13}$$

where $I_0(z)$ is the Bessel function of imaginary argument.

Finally, we should take into account that in the experiment of Ref. [50] the upper test body was not a sinusoidally corrugated plate, but a sinusoidally corrugated sphere. The force $F_{\text{corr}}^{(s,p)}$ acting between a corrugated spherical envelope of thickness d_2 and a corrugated plate can be expressed via the energy per unit area of two corrugated plates (13) by means of the proximity force approximation (PFA) [60, 61]

$$F_{\text{corr}}^{(s,p)}(a) = 2\pi R E_{\text{corr}}(a). \tag{14}$$

The PFA is sufficiently exact under the condition $a \ll R$ (in this case its error is less than a/R for the Casimir force [62–65] and takes much less values for the exponentially decreasing forces, such as the Yukawa force and the force due to two-axion exchange). One more condition for the validity of Eq. (14) in application to forces due to the exchange of scalar or pseudoscalar particles is that the Compton wavelength of a hypothetical particle should be much less than the sphere radius, i.e., $1/m_a \ll R$ [66, 67]. This is also satisfied in our case taking into account that the competitive constraints from the experiment of Ref. [50] follow for $m_a > 1 \text{ eV}$ ($1/m_a < 200 \text{ nm}$). For the validity of Eq. (14) in the case of a spherical envelope, its thickness should be sufficiently small, i.e., $d_2 \ll R$ [66, 67]. As a result, Eqs. (13) and (14) provide an analytic expression for the force due to the exchange of two axion-like particles acting between a sinusoidally corrugated spherical envelope of radius R and thickness d_2 and a sinusoidally corrugated plate of thickness d_1 .

B. Derivation of constraints

Now we take into account that in the experiment of Ref. [50] the plate was coated with an Au layer and the polystyrene sphere was coated with layers of Cr, Al and Au, with the densities $\rho_{\text{Cr}} = 7.15 \text{ g/cm}^3$, $\rho_{\text{Al}} = 2.7 \text{ g/cm}^3$, and $\rho_{\text{Au}} = 19.29 \text{ g/cm}^3$, respectively. Note that the hard epoxy and polystyrene are materials of low density and lead to negligibly small

contributions to the force due to exchange of two axion-like particles. By applying Eqs. (13) and (14) to each pair of metallic layers (the inequalities $\Delta_{\text{Cr}}^{(2)}, \Delta_{\text{Al}}^{(2)}, \Delta_{\text{Au}}^{(2)} \ll R$ are satisfied with a large safety margin), the resulting expression for the force due to two-axion exchange in the experimental configuration of Ref. [50] takes the form

$$\begin{aligned}
F_{\text{corr}}^{(s,p)}(a) = & -\frac{\pi R C_{\text{Au}}}{2m_a m^2 m_{\text{H}}^2} \int_1^\infty du \frac{\sqrt{u^2 - 1}}{u^3} e^{-2m_a u a} \\
& \times I_0(2m_a u (A_1 - A_2)) (1 - e^{-2m_a u \Delta_{\text{Au}}^{(1)}}) \\
& \times \left[C_{\text{Au}} + (C_{\text{Al}} - C_{\text{Au}}) e^{-2m_a u \Delta_{\text{Au}}^{(2)}} \right. \\
& + (C_{\text{Cr}} - C_{\text{Al}}) e^{-2m_a u (\Delta_{\text{Au}}^{(2)} + \Delta_{\text{Al}}^{(2)})} \\
& \left. - C_{\text{Cr}} e^{-2m_a u (\Delta_{\text{Au}}^{(2)} + \Delta_{\text{Al}}^{(2)} + \Delta_{\text{Cr}}^{(2)})} \right]. \tag{15}
\end{aligned}$$

Here, the coefficients C_{Au} , C_{Al} , and C_{Cr} are defined according to Eq. (7), as applied to respective elements. The quantities Z/μ and N/μ are equal to [56] 0.40422 and 0.60378, 0.48558 and 0.52304, 0.46518 and 0.54379 for Au, Al, and Cr, respectively.

The Casimir force between a corrugated sphere and a corrugated plate was measured at separations $a \geq 127$ nm and found to be in good agreement with theoretical predictions of the scattering theory [50]. This theory is a generalization of the Lifshitz theory of the van der Waals and Casimir forces for the case of boundary surfaces of arbitrary shape [68]. It should be noted that there is a problem in theory-experiment comparison connected with different models for the low-frequency behavior of the dielectric permittivity [60, 61]. It turned out that the measurement data of the most precise experiments using a metal-coated sphere above a metal-coated plate agree with theoretical predictions only if the relaxation of conduction electrons is omitted (in so doing the relaxation properties of bound electrons are taken into account). At separation distances of a few hundred nanometers the effect of relaxation of free electrons comes to only several percent. However, the theoretical predictions taking this kind of relaxation into account were reliably excluded in the dynamic experiments performed by means of AFM [40–44] and micromachined oscillator [45, 46].

Luckily, this problem is unrelated to experiments with corrugated surfaces under consideration here. The point is that they are performed by means of AFM at shorter separation distances where the dynamic mode is inoperable. As a result, in the static mode, the experimental error in force measurements exceeds the theoretical uncertainty connected with an account or neglect of the relaxation properties of free charge carriers.

As was noted above, the measurement data of Ref. [50] were found to be in a good agreement with theoretical predictions for the Casimir force. No signature of any other interaction, specifically, due to exchange of two axion-like particles was found in the limits of the total experimental error, $\Delta F_C^{(s,p)}(a)$, in the measured Casimir force. This error was determined at the 67% confidence level as a combination of random and systematic errors. Thus, one can conclude that any additional force between the sphere and the plate, specifically, arising due to two-axion exchange should satisfy the inequality

$$|F_{\text{corr}}^{(s,p)}(a)| \leq \Delta F_C^{(s,p)}(a), \quad (16)$$

where the left-hand side is given in Eq. (15). We have analyzed Eq. (16) numerically and found that the strongest constraints on the coupling constants g_{an} , g_{ap} as functions of m_a follow at the shortest separation $a = 127$ nm. At this separation distance the total experimental error determined at the 67% confidence level is $\Delta F_C^{(s,p)}(a) = 0.94$ pN [50]. Then, the constraints following from Eq. (16) are also determined at the same 67% confidence level. Note that the constraints obtained in this way are the conservative ones. The inclusion of any unaccounted attractive force between a sphere and a plate, in addition to the force due to two-axion exchange, could make them only stronger.

In Fig. 1(a) we show the constraints on the constants $g_{ap(n)}^2/(4\pi)$ as functions of m_a obtained from Eq. (16) at $a = 127$ nm. The three lines from bottom to top corresponding to the equality sign in Eq. (16) are plotted under the conditions $g_{ap}^2 = g_{an}^2$, $g_{an}^2 \gg g_{ap}^2$, and $g_{ap}^2 \gg g_{an}^2$, respectively. The regions of the plane above each line are prohibited by the measurement results and below each line are allowed. The range of masses of axion-like particles from 1 eV to 20 eV is chosen. For larger m_a the strength of the constraints shown in Fig. 1(a) decreases quickly. This is in line with the constraints on the Yukawa-type interactions obtained in Ref. [59] from the same experiment. The strongest constraints on the Yukawa interaction constant were found in the interaction range from 15 to 65 nm [59], which corresponds to the mass of a hypothetical scalar particle from 2 to 15 eV.

In Fig. 1(b) the constraints derived here under the condition $g_{ap}^2 = g_{an}^2$ [the black line reproducing the lower line of Fig. 1(a)] are compared with the strongest constraints obtained [38] under the same condition from measuring the Casimir pressure by means of micromachined oscillator [45, 46] (the gray line). As is seen in Fig. 1(b), the constraints obtained here are stronger in the region of masses of axion-like particles $m_a \geq 11$ eV.

III. CONSTRAINTS FROM MEASURING THE LATERAL CASIMIR FORCE BETWEEN SINUSOIDALLY CORRUGATED SURFACES

In Refs. [51, 52] the lateral Casimir force was measured by means of AFM as a function of the phase shift φ_0 between uniaxial corrugations of period $\Lambda = 574.4$ nm on the sphere and on the plate over the region of separations from $a = 120$ nm to $a = 190$ nm. The corrugation amplitudes on the plate and on the sphere were $A_1 = 85.4$ nm and $A_2 = 13.7$ nm, respectively. The top of the plate (the grating made of a hard epoxy) was covered with $\Delta_{\text{Au}}^{(1)} = 300$ nm Au coating. The sphere was made of polystyrene and coated with a layer of Cr of $\Delta_{\text{Cr}}^{(2)} = 10$ nm and then with a layer of Au of $\Delta_{\text{Au}}^{(2)} = 50$ nm thickness. The outer radius of the coated sphere was measured to be $R = 97.0$ μm . Unlike the experiment of Ref. [50] considered in Sec. II, the corrugation axes on the plate and on the sphere were always parallel, but the phase shift between corrugations was varied leading to a nonzero lateral Casimir force.

A. Calculation of the lateral force due to exchange of two axion-like particles

Now we calculate the lateral force (acting in tangential directions to the mean levels of boundary surfaces) between the sinusoidally corrugated spherical envelope of thickness d_2 and the sinusoidally corrugated plate of thickness d_1 , which arises due to two-axion exchange.

Similarly to Sec. IIA, we consider first two plane parallel plates with thicknesses d_1 and d_2 and again arrive at the interaction energy per unit area due to two-axion exchange given by Eq. (9). Then we assume that the opposite sides of the plates are covered with uniaxial sinusoidal corrugations of an equal period but with some phase shift $\varphi = 2\pi x_0/\Lambda$. As a result, the separation distance between the surfaces of the plates is given not by Eq. (10), but by the following expressions:

$$z \equiv z(x) = a + A_1 \cos \frac{2\pi x}{\Lambda} - A_2 \cos \frac{2\pi(x + x_0)}{\Lambda}. \quad (17)$$

Equation (17) can be identically rearranged to

$$z = a + b \cos \left(\frac{2\pi x}{\Lambda} + \tilde{\varphi} \right), \quad (18)$$

where

$$b = (A_1^2 + A_2^2 - 2A_1A_2 \cos \varphi)^{1/2},$$

$$\cot \tilde{\varphi} = \frac{A_1 - A_2 \cos \varphi}{A_2 \sin \varphi}. \quad (19)$$

Substituting Eqs. (9) and (18) in Eq. (11) and integrating with respect to x , we obtain

$$E_{\text{corr}}(a) = -\frac{C_1 C_2}{4m_a m^2 m_H^2} \int_1^\infty du \frac{\sqrt{u^2 - 1}}{u^3}$$

$$\times e^{-2m_a u a} I_0(2m_a u b)$$

$$\times (1 - e^{-2m_a u d_1})(1 - e^{-2m_a u d_2}). \quad (20)$$

This is the generalization of Eq. (13) for the case of a nonzero phase shift between corrugations on both surfaces.

Using the PFA in Eq. (14), we now find the normal force due to exchange of two axion-like particles acting between a sinusoidally corrugated spherical envelope of thickness d_2 and a sinusoidally corrugated plate of thickness d_1

$$F_{\text{corr}}^{(s,p)}(a) = -\frac{\pi R C_1 C_2}{2m_a m^2 m_H^2} \int_1^\infty du \frac{\sqrt{u^2 - 1}}{u^3}$$

$$\times e^{-2m_a u a} I_0(2m_a u b)$$

$$\times (1 - e^{-2m_a u d_1})(1 - e^{-2m_a u d_2}). \quad (21)$$

This approximate expression is applicable under the conditions $a \ll R$, $1/m_a \ll R$, and $d_2 \ll R$ (see Sec. IIA).

By the negative integration of Eq. (21) with respect to a , one can obtain the interaction energy due to two-axion exchange between the corrugated sphere and the corrugated plate

$$E_{\text{corr}}^{(s,p)}(a) = -\frac{\pi R C_1 C_2}{4m_a^2 m^2 m_H^2} \int_1^\infty du \frac{\sqrt{u^2 - 1}}{u^4}$$

$$\times e^{-2m_a u a} I_0(2m_a u b)$$

$$\times (1 - e^{-2m_a u d_1})(1 - e^{-2m_a u d_2}). \quad (22)$$

Then, the lateral force due to exchange of two axion-like particles is obtained by the negative

differentiation of Eq. (22) with respect to the phase shift between corrugations

$$\begin{aligned}
F_{\text{corr, lat}}^{(s,p)}(a) &= -\frac{\partial E_{\text{corr}}^{(s,p)}(a)}{\partial x_0} = -\frac{2\pi}{\Lambda} \frac{\partial E_{\text{corr}}^{(s,p)}(a)}{\partial \varphi} \\
&= \frac{\pi^2 R C_1 C_2}{m_a m^2 m_H^2} \frac{A_1 A_2}{b \Lambda} \sin \varphi \int_1^\infty du \frac{\sqrt{u^2 - 1}}{u^3} \\
&\quad \times e^{-2m_a u a} I_1(2m_a u b) \\
&\quad \times (1 - e^{-2m_a u d_1})(1 - e^{-2m_a u d_2}).
\end{aligned} \tag{23}$$

This expression can be used for constraining the parameters of axion-like particles from the experimental data of Refs. [51, 52].

B. Constraints from measuring the lateral Casimir force

To obtain the constraints on axion-like particles from the experimental data, it is necessary to take into account the layer structure of the test bodies. Similarly to Sec. IIB, the hard epoxy and polystyrene lead to negligibly small contributions to the force due to two-axion exchange. Thus, one should take into account the Au layer on the plate, and Cr and Au layers on the sphere. The resulting lateral force is found by applying Eq. (23) two times. We also take into account that the largest magnitude of the lateral force due to two-axion exchange and, as a consequence, strongest constraints are obtained for the phase shift $\varphi = \pi/2$, $b = \sqrt{A_1^2 + A_2^2}$. In this case

$$\begin{aligned}
\max |F_{\text{corr, lat}}^{(s,p)}(a)| &= \frac{\pi^2 R C_{\text{Au}}}{m_a m^2 m_H^2} \frac{A_1 A_2}{\Lambda \sqrt{A_1^2 + A_2^2}} \\
&\quad \times \int_1^\infty du \frac{\sqrt{u^2 - 1}}{u^3} e^{-2m_a u a} I_1 \left(2m_a u \sqrt{A_1^2 + A_2^2} \right) \\
&\quad \times (1 - e^{-2m_a u \Delta_{\text{Au}}^{(1)}}) \left[C_{\text{Au}} + (C_{\text{Cr}} - C_{\text{Au}}) \right. \\
&\quad \left. \times e^{-2m_a u \Delta_{\text{Au}}^{(2)}} - C_{\text{Cr}} e^{-2m_a u (\Delta_{\text{Au}}^{(2)} + \Delta_{\text{Cr}}^{(2)})} \right].
\end{aligned} \tag{24}$$

Similarly to the experiment of Ref. [50] discussed in Sec. II, the measurement data for the lateral Casimir force were found to be in a good agreement with theoretical predictions of the scattering theory. No additional lateral force was observed in Refs. [51, 52] in the limits of the total experimental error $\Delta F_{C, \text{lat}}^{(s,p)}(a)$ in the measured lateral Casimir force. The theoretical uncertainty due to an account or neglect of the relaxation properties of free

charge carriers is again smaller than this error. Because of this, the force due to exchange of two axion-like particles is constrained by the inequality

$$\max |F_{\text{corr, lat}}^{(s,p)}(a)| \leq \Delta F_{C, \text{lat}}^{(s,p)}(a), \quad (25)$$

where the left-hand side is given by Eq. (24). The strongest constraints for axion-like particles with $m_a \leq 20$ eV are obtained from the measurement data at $a = 124.7$ nm where the total experimental error is $\Delta F_{C, \text{lat}}^{(s,p)}(a) = 4.7$ pN [51, 52]. This error was determined at a higher, 95%, confidence level. Thus, the reliability of the obtained constraints is also characterized by the 95% confidence level.

The constraints on the constants $g_{ap(n)}^2/(4\pi)$ following from Eq. (25) are shown in Fig. 2(a) as functions of the axion mass. The three lines from bottom to top are plotted under the conditions $g_{ap}^2 = g_{an}^2$, $g_{an}^2 \gg g_{ap}^2$, and $g_{ap}^2 \gg g_{an}^2$, respectively. As in Fig. 1(a), the regions of the plane above each line are prohibited and below each line are allowed. The same range of masses of axion-like particles $1 \text{ eV} \leq m_a \leq 20 \text{ eV}$ is chosen. For larger masses the strength of the obtained constraints quickly decreases.

In Fig. 2(b) we compare the constraints derived here under the condition $g_{ap}^2 = g_{an}^2$ [the black solid line reproducing the lower line from Fig. 2(a)] with the strongest constraints derived in Sec. IIB from measurements of the normal Casimir force [the dashed line reproducing the lower line from Fig. 1(a)] and derived in Ref. [38] from measurements of the Casimir pressure by means of micromachined oscillator [the gray solid line reproducing the similar line from Fig. 1(b)]. As is seen in Fig. 2(b), the constraints obtained here from measurements of the lateral Casimir force are stronger than those from measurements of the normal Casimir force for $m_a \geq 5$ eV and stronger than the constraints following from measurements of the Casimir pressure by means of micromachined oscillator for $m_a \geq 8$ eV.

IV. COMPARISON BETWEEN DIFFERENT MODEL-INDEPENDENT CONSTRAINTS

Many constraints on the parameters of axions and axion-like particles were obtained with the help of some model approaches. As discussed in Sec. I, within the model of hadronic axions, whose coupling constant is a function of m_a , the upper limits for the axion mass $m_a \leq 159$ eV [20] and $m_a \leq 145$ eV [21] were obtained using the detector of γ -quanta

appearing in the deexcitation of the nuclear level excited by solar axions. The parameters of hadronic axions were also found from the neutrino data of supernova SN 1987A [22] and from astrophysical arguments connected with stellar cooling by the axion emission [23, 24]. In so doing, some model description of dense nuclear matter was used [24]. Here, we collect the model-independent constraints on the coupling constants of axion-like particles to nucleons which were obtained from table-top laboratory experiments and are relevant to different models of axions.

In Fig. 3 the constraints on the coupling constant of axion-like particles to neutrons as functions of m_a are shown over the wide range of axion masses from 10^{-10} eV to 20 eV. The solid line 1 in Fig. 3 shows the constraints obtained [28] by means of a magnetometer using spin-polarized K and ^3He atoms. These constraints are found in the region from 10^{-10} eV to 6×10^{-6} eV. The constraints obtained [34] from the modern Cavendish-type experiment [35] in the region from $m_a = 10^{-6}$ eV to 6×10^{-2} eV are shown by the solid line 2. The dashed lines 3 and 4 indicate the weaker constraints found in Ref. [29] from the older Cavendish-type experiments [32, 33] and from the Eötvös-type experiment [30], respectively. These constraints extend from $m_a = 10^{-8}$ eV to $m_a = 4 \times 10^{-5}$ (line 3) and to 10^{-5} eV (line 4). They are obtained under the assumption that $g_{an} = g_{ap}$. All the constraints indicated by the lines 5–8 are also obtained under this assumption. The solid line 5 found in the region from 10^{-3} to 15 eV follows [38] from measurements of the Casimir pressure by means of micromachined oscillator, the dashed line 6 was obtained [37] in the region from 3×10^{-5} to 1 eV from measuring the gradient of the Casimir force by means of dynamic AFM [40, 41], and the dashed line 7 was found [36] in the region from 10^{-4} to 0.3 eV from the experiment on measuring the Casimir-Polder force [39]. Finally, the solid line 8 indicates the constraints obtained here in the region of masses of axion-like particles from 1 to 20 eV from measuring the lateral Casimir force between corrugated surfaces (as shown in Sec. IIB, the experiment of Ref. [50] on measuring the normal Casimir force in the same configuration leads to slightly weaker constraints). The region above each line in Fig. 3 is prohibited by the results of respective experiment whereas the region below each line is allowed.

As can be seen in Fig. 3, the strength of laboratory constraints on the axion to nucleon coupling constants decreases with increasing axion mass. The same is true for the Yukawa-type corrections to Newtonian gravitational law which arise due to exchange of light scalar particles between atoms and molecules of interacting bodies (see Ref. [60] for a review and

Refs. [58, 59, 69–72] for the most recent results). In fact, for both additional interactions (due to the exchange of pseudoscalar and scalar particles, respectively) the gravitational experiments of Eötvös and Cavendish type lead to strongest constraints within the moderately short interaction regions (moderately large masses). For shorter interaction regions (larger masses) stronger constraints are obtained from measurements of the Casimir and Casimir-Polder forces [58, 59, 69–72]. This is illustrated in Fig. 3, where the constraints on couplings of axion-like particles to nucleons obtained from the Casimir effect become stronger than those obtained from the gravitational experiments for $m_a \geq 2 \times 10^{-3}$ eV.

There are other purely laboratory experiments setting strong constraints on the coupling constants of axion-like particles with larger m_a to nucleons. Recently such constraints have been obtained [73] from the comparison of nuclear magnetic resonance measurements with calculations of the scalar spin-spin interaction in deuterated molecular hydrogen. The combination of the coupling constants $g_{ap}(g_{ap} + g_{an})/(4\pi)$ was shown to be less than 3.6×10^{-7} for m_a in the range of 5×10^3 eV.

V. CONCLUSIONS AND DISCUSSION

In this paper, we have obtained constraints on the coupling constants of axion-like particles to nucleons from measuring the normal and lateral Casimir force between sinusoidally corrugated Au-coated surfaces of a sphere and a plate [50–52] by means of AFM. These constraints are obtained from the measure of agreement between the measured and calculated Casimir forces. It is worth noting that calculation of the Casimir interaction between arbitrarily shaped test bodies is a complicated theoretical problem which was solved recently using the quantum-field theoretical formalism of functional determinants and scattering amplitudes [68]. Taking into account that the test bodies in the experiments of Refs. [50–52] are unpolarized, there is no any additional force due to an exchange of one axion between protons and neutrons. There is, however, the additional force between corrugated surfaces arising due to exchange of two axion-like particles, and it is constrained by the magnitude of the experimental error in measurements of the Casimir force.

We have calculated both the normal and lateral forces due to exchange of two axion-like particles between protons and neutrons of sinusoidally corrugated surfaces of a sphere and a plate. The respective model-independent constraints on the coupling constants of

axion-like particles to protons and to neutrons were obtained for the region of masses from 1 eV to 20 eV. It was shown that the experiment of Ref. [50] on measuring the normal Casimir force leads to the strongest constraints on the coupling constants $g_{ap(n)}$ for masses of axion-like particles $m_a \geq 11$ eV. In this region of m_a , the constraints obtained here are stronger than those following from measurements of the effective Casimir pressure by means of micromachined oscillator [38]. We have obtained even stronger constraints on the coupling constants of axion-like particles to nucleons from the experiment of Refs. [51, 52], where the lateral Casimir force between sinusoidally corrugated surfaces has been measured. These constraints are stronger than those found from measurements using a micromachined oscillator in the region of masses of axion-like particles $m_a \geq 8$ eV.

The obtained constraints were compared with other laboratory constraints on the coupling constants of axions to nucleons found in different experiments. We have considered constraints following from the magnetometer measurements with polarized atoms [28], from the experiments of Eötvös type [29–31], different experiments of Cavendish type [29, 32, 33, 35], and from various measurements of the Casimir interaction [39–41, 45, 46, 51, 52]. These constraints cover the wide range of masses of axion-like particles from 10^{-10} eV to 20 eV.

In future, it seems promising to perform measurements of the Casimir interaction between polarized (magnetized) test bodies. In this case, the process of a one-axion exchange between nucleons would contribute to the additional force and result in much stronger constraints on the coupling constants of axion-like particles to nucleons.

Acknowledgments

The authors of this work acknowledge CNPq (Brazil) for partial financial support. G.L.K. and V.M.M. are grateful to U. Mohideen for useful information about his experiments and to M. I. Eides for helpful discussions. They also acknowledge the Department of Physics of the Federal University of Paraíba (João Pessoa, Brazil) for hospitality.

-
- [1] R. D. Peccei and H. R. Quinn, *Phys. Rev. Lett.* **38**, 1440 (1977).
 - [2] S. Weinberg, *Phys. Rev. Lett.* **40**, 223 (1978).
 - [3] F. Wilczek, *Phys. Rev. Lett.* **40**, 279 (1978).

- [4] J. E. Kim, Phys. Rep. **150**, 1 (1987).
- [5] Yu. N. Gnedin, Int. J. Mod. Phys. A **17**, 4251 (2002).
- [6] L. J. Rosenberg and K. A. van Bibber, Phys. Rep. **325**, 1 (2000).
- [7] G. G. Raffelt, J. Phys. A: Math. Theor. **40**, 6607 (2007).
- [8] J. E. Kim and G. Carosi, Rev. Mod. Phys. **82**, 557 (2010).
- [9] J. Beringer *et al.* (Particle Data Group), Phys. Rev. D **86**, 010001 (2012).
- [10] K. Baker *et al.* Ann. Phys. (Berlin) **525**, A93 (2013).
- [11] A. R. Zhitnitskii, Sov. J. Nucl. Phys. **31**, 260 (1980).
- [12] M. Dine, F. Fischler, and M. Srednicki, Phys. Lett. B **104**, 199 (1981).
- [13] J. E. Kim, Phys. Rev. Lett. **43**, 103 (1979).
- [14] M. A. Shifman, A. I. Vainshtein, and V. I. Zakharov, Nucl. Phys. B **166**, 493 (1980).
- [15] Z. G. Berezhiani and M. Yu. Khlopov, Z.Phys. C — Particles and Fields **49**, 73 (1991).
- [16] M. Khlopov, *Fundamentals of Cosmic Particle Physics* (CISP-Springer, Cambridge, 2012).
- [17] M. Arik *et al.*, Phys. Rev. Lett. **107**, 261302 (2011).
- [18] G. G. Raffelt, Phys. Rev. D **33**, 897 (1986).
- [19] H. Schlattl, A. Weiss, and G. Raffelt, Astropart. Phys. **10**, 353 (1999).
- [20] A. V. Derbin, A. L. Frolov, L. A. Mitropol'sky, V. N. Muratova, D. A. Semenov, and E. V. Unzhakov, Eur. Phys. J. C **62**, 755 (2009).
- [21] A. V. Derbin, V. N. Muratova, D. A. Semenov, and E. V. Unzhakov, Phys. Atom. Nucl. **74**, 596 (2011).
- [22] J. Engel, D. Seckel, and A. C. Hayes, Phys. Rev. Lett. **65**, 960 (1990).
- [23] W. C. Haxton and K. Y. Lee, Phys. Rev. Lett. **66**, 2557 (1991).
- [24] G. Raffelt, Phys. Rev. D **86**, 015001 (2012).
- [25] E. Massó and J. Redondo, Phys. Rev. Lett. **97**, 151802 (2006).
- [26] J. Jaeckel, E. Massó, J. Redondo, A. Ringwald, and F. Takahashi, Phys. Rev. D **75**, 013004 (2007).
- [27] P. Brax, C. van de Bruck, and A.-C. Davis, Phys. Rev. Lett. **99**, 121103 (2007).
- [28] G. Vasilakis, J. M. Brown, T. R. Kornack, and M. V. Romalis, Phys. Rev. Lett. **103**, 261801 (2009).
- [29] E. G. Adelberger, E. Fischbach, D. E. Krause, and R. D. Newman, Phys. Rev. D **68**, 062002 (2003).

- [30] G. L. Smith, C. D. Hoyle, J. H. Gundlach, E. G. Adelberger, B. R. Heckel, and H. E. Swanson, Phys. Rev. D **61**, 022001 (1999).
- [31] J. H. Gundlach, G. L. Smith, E. G. Adelberger, B. R. Heckel, and H. E. Swanson, Phys. Rev. Lett. **78**, 2523 (1997).
- [32] R. Spero, J. K. Hoskins, R. Newman, J. Pellam, and J. Schultz, Phys. Rev. Lett. **44**, 1645 (1980).
- [33] J. K. Hoskins, R. D. Newman, R. Spero, and J. Schulz, Phys. Rev. D **32**, 3084 (1985).
- [34] E. G. Adelberger, B. R. Heckel, S. Hoedl, C. D. Hoyle, D. J. Kapner, and A. Upadhye, Phys. Rev. Lett. **98**, 131104 (2007).
- [35] D. J. Kapner, T. S. Cook, E. G. Adelberger, J. H. Gundlach, B. R. Heckel, C. D. Hoyle, and H. E. Swanson, Phys. Rev. Lett. **98**, 021101 (2007).
- [36] V. B. Bezerra, G. L. Klimchitskaya, V. M. Mostepanenko, and C. Romero, Phys. Rev. D **89**, 035010 (2014).
- [37] V. B. Bezerra, G. L. Klimchitskaya, V. M. Mostepanenko, and C. Romero, Phys. Rev. D **89**, 075002 (2014).
- [38] V. B. Bezerra, G. L. Klimchitskaya, V. M. Mostepanenko, and C. Romero, Eur. Phys. J. C **74**, 2859 (2014).
- [39] J. M. Obrecht, R. J. Wild, M. Antezza, L. P. Pitaevskii, S. Stringari, and E. A. Cornell, Phys. Rev. Lett. **98**, 063201 (2007).
- [40] C.-C. Chang, A. A. Banishev, R. Castillo-Garza, G. L. Klimchitskaya, V. M. Mostepanenko, and U. Mohideen, Phys. Rev. B **85**, 165443 (2012).
- [41] A. A. Banishev, C.-C. Chang, R. Castillo-Garza, G. L. Klimchitskaya, V. M. Mostepanenko, and U. Mohideen, Int. J. Mod. Phys. A **27**, 1260001 (2012).
- [42] A. A. Banishev, C.-C. Chang, G. L. Klimchitskaya, V. M. Mostepanenko, and U. Mohideen, Phys. Rev. B **85**, 195422 (2012).
- [43] A. A. Banishev, G. L. Klimchitskaya, V. M. Mostepanenko, and U. Mohideen, Phys. Rev. Lett. **110**, 137401 (2013).
- [44] A. A. Banishev, G. L. Klimchitskaya, V. M. Mostepanenko, and U. Mohideen, Phys. Rev. B **88**, 155410 (2013).
- [45] R. S. Decca, D. López, E. Fischbach, G. L. Klimchitskaya, D. E. Krause, and V. M. Mostepanenko, Phys. Rev. D **75**, 077101 (2007).

- [46] R. S. Decca, D. López, E. Fischbach, G. L. Klimchitskaya, D. E. Krause, and V. M. Mostepanenko, Eur. Phys. J. C **51**, 963 (2007).
- [47] H. B. Chan, Y. Bao, J. Zou, R. A. Cirelli, F. Klemens, W. M. Mansfield, and C. S. Pai, Phys. Rev. Lett. **101**, 030401 (2008).
- [48] Y. Bao, R. Guérout, J. Lussange, A. Lambrecht, R. A. Cirelli, F. Klemens, W. M. Mansfield, C. S. Pai, and H. B. Chan, Phys. Rev. Lett. **105**, 250402 (2010).
- [49] R. Guérout, J. Lussange, H. B. Chan, A. Lambrecht, and S. Reynaud, Phys. Rev. A **87**, 052514 (2013).
- [50] A. A. Banishev, J. Wagner, T. Emig, R. Zandi, and U. Mohideen, Phys. Rev. Lett. **110**, 250403 (2013).
- [51] H.-C. Chiu, G. L. Klimchitskaya, V. N. Marachevsky, V. M. Mostepanenko, and U. Mohideen, Phys. Rev. B **80**, 121402(R) (2009).
- [52] H.-C. Chiu, G. L. Klimchitskaya, V. N. Marachevsky, V. M. Mostepanenko, and U. Mohideen, Phys. Rev. B **81**, 115417 (2010).
- [53] J. E. Moody and F. Wilczek, Phys. Rev. D **30**, 130 (1984).
- [54] S. D. Drell and K. Huang, Phys. Rev. **91**, 1527 (1953).
- [55] F. Ferrer and M. Nowakowski, Phys. Rev. D **59**, 075009 (1999).
- [56] E. Fischbach and C. L. Talmadge, *The Search for Non-Newtonian Gravity* (Springer, New York, 1999).
- [57] I. S. Gradshteyn and I. M. Ryzhik, *Table of Integrals, Series and Products* (Academic Press, New York, 1980).
- [58] V. B. Bezerra, G. L. Klimchitskaya, V. M. Mostepanenko, and C. Romero, Phys. Rev. D **81**, 055003 (2010).
- [59] G. L. Klimchitskaya, U. Mohideen, and V. M. Mostepanenko, Phys. Rev. D **87**, 125031 (2013).
- [60] M. Bordag, G. L. Klimchitskaya, U. Mohideen, and V. M. Mostepanenko, *Advances in the Casimir Effect* (Oxford University Press, Oxford, 2009).
- [61] G. L. Klimchitskaya, U. Mohideen, and V. M. Mostepanenko, Rev. Mod. Phys. **81**, 1827 (2009).
- [62] C. D. Fosco, F. C. Lombardo, F. D. Mazzitelli, Phys. Rev. D **84**, 105031 (2011).
- [63] G. Bimonte, T. Emig, R. L. Jaffe, M. Kardar, Europhys. Lett. **97**, 50001 (2012).
- [64] G. Bimonte, T. Emig, M. Kardar, Appl. Phys. Lett. **100**, 074110 (2012).

- [65] L. P. Teo, Phys. Rev. D **88**, 045019 (2013).
- [66] R. S. Decca, E. Fischbach, G. L. Klimchitskaya, D. E. Krause, D. López, V. M. Mostepanenko, Phys. Rev. D **79**, 124021 (2009).
- [67] E. Fischbach, G. L. Klimchitskaya, D. E. Krause, V. M. Mostepanenko, Eur. Phys. J. C **68**, 223 (2010).
- [68] S. J. Rahi, T. Emig, N. Graham, R. L. Jaffe, and M. Kardar, Phys. Rev. D **80**, 085021 (2009).
- [69] V. B. Bezerra, G. L. Klimchitskaya, V. M. Mostepanenko, and C. Romero, Phys. Rev. D **83**, 075004 (2011).
- [70] G. L. Klimchitskaya, U. Mohideen, and V. M. Mostepanenko, Phys. Rev. D **86**, 065025 (2012).
- [71] V. M. Mostepanenko, V. B. Bezerra, G. L. Klimchitskaya, and C. Romero, Int. J. Mod. Phys. A **27**, 1260015 (2012).
- [72] G. L. Klimchitskaya and V. M. Mostepanenko, Grav. Cosmol. **20**, 3 (2014).
- [73] M. P. Ledbetter, M. V. Romalis, and D. F. J. Kimball, Phys. Rev. Lett. **110**, 040402 (2013).

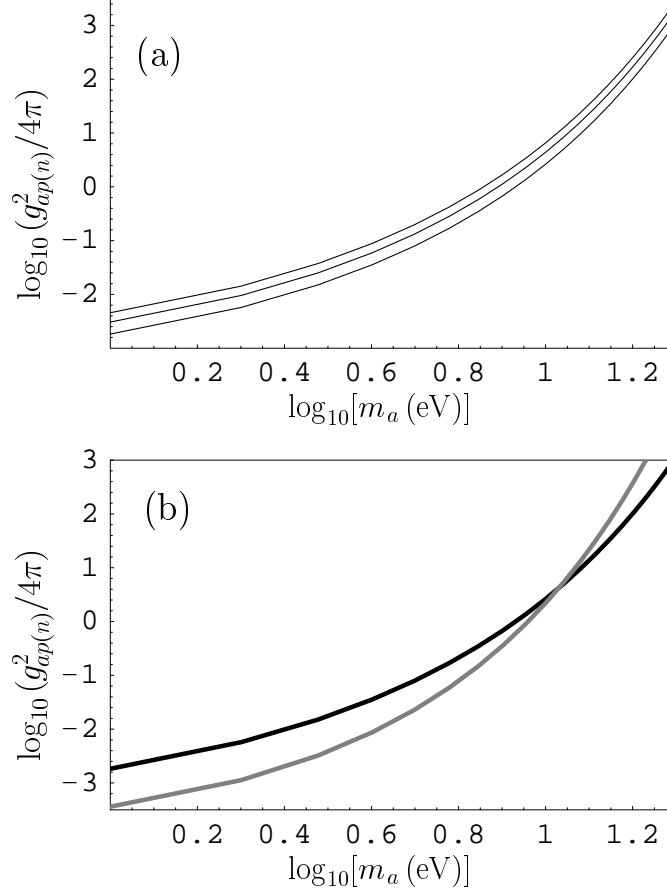


FIG. 1: Constraints on the coupling constants of axion-like particles to nucleons are shown as functions of the axion mass. The regions above each line are prohibited and below each line are allowed. (a) Constraints from measurements of the normal Casimir force between corrugated surfaces of a sphere and a plate. The lines from bottom to top are plotted under the conditions $g_{ap}^2 = g_{an}^2$, $g_{an}^2 \gg g_{ap}^2$, and $g_{ap}^2 \gg g_{an}^2$, respectively. (b) Constraints from measurements of the normal Casimir force between corrugated surfaces of a sphere and a plate and from the experiment using a micromachined oscillator are plotted under the condition $g_{ap}^2 = g_{an}^2$ by the black and gray lines, respectively.

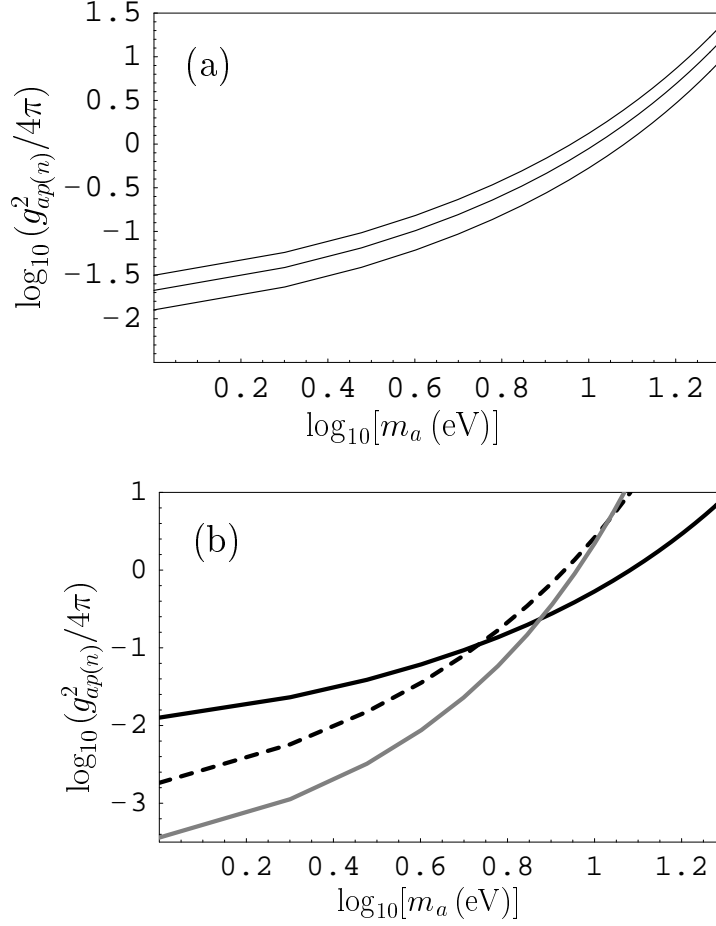


FIG. 2: Constraints on the coupling constants of axion-like particles to nucleons are shown as functions of the axion mass. The regions above each line are prohibited and below each line are allowed. (a) Constraints from measurements of the lateral Casimir force between corrugated surfaces of a sphere and a plate. The lines from bottom to top are plotted under the conditions $g_{ap}^2 = g_{an}^2$, $g_{an}^2 \gg g_{ap}^2$, and $g_{ap}^2 \gg g_{an}^2$, respectively. (b) Constraints from measurements of the lateral and normal Casimir force between corrugated surfaces of a sphere and a plate are plotted under the condition $g_{ap}^2 = g_{an}^2$ by the solid and dashed black lines, respectively. The constraints from measuring the Casimir pressure by means of micromachined oscillator are shown by the gray line.

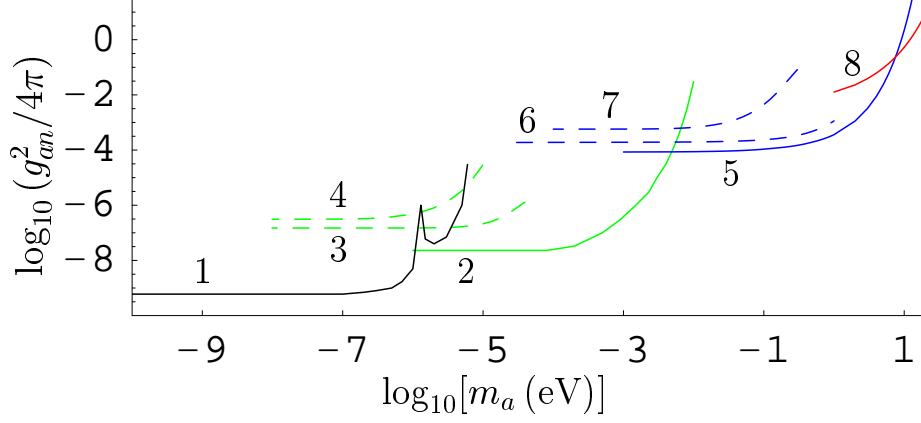


FIG. 3: (Color online) The laboratory constraints on the coupling constants of axion-like particles to a neutron obtained from different experiments are shown by the lines 1–8 as functions of the axion mass. The line 1 follows from the magnetometer measurements [28]. The lines 2–4 are found [29, 34] from the gravitational experiments [30–33, 35], and the lines 5–8 are obtained in Refs. [36–38] and in this paper from the Casimir effect [39–41, 45, 46, 51, 52] (see text for further discussion). The regions above each line are prohibited and below each line are allowed.